Raman Lasing with a Cold Atom Gain Medium in a High-Finesse Optical Cavity

Geert Vrijsen, Onur Hosten, Jongmin Lee, Simon Bernon,* and Mark A. Kasevich

Physics Department, Stanford University, Stanford, California 94305, USA

(Received 24 December 2010; revised manuscript received 6 May 2011; published 4 August 2011)

We demonstrate a Raman laser using cold ^{87}Rb atoms as the gain medium in a high-finesse optical cavity. We observe robust continuous wave lasing in the atypical regime where single atoms can considerably affect the cavity field. Consequently, we discover unusual lasing threshold behavior in the system causing jumps in lasing power, and propose a model to explain the effect. We also measure the intermode laser linewidth, and observe values as low as 80 Hz. The tunable gain properties of this laser suggest multiple directions for future research.

DOI: 10.1103/PhysRevLett.107.063904 PACS numbers: 42.55.Ye

Ultrahigh-precision spectroscopy, metrology, and many quantum optics experiments stand to benefit substantially from the advance of gain media that can be tuned for properties like gain bandwidth, index of refraction, or dispersion. Raman gain in atomic systems permits precise control over such properties through variations in the pumping mechanism. Recent experiments in heated atomic vapors, pumped by light at two optical frequencies, for instance, demonstrate anomalous dispersion [1]. Such a property could be integrated into a lasing system to increase sensitivity of lasing frequency to the laser cavity length, e.g., to enhance gravity wave detection sensitivity. As another example, Raman gain allows the tunability of the effective dipole moments of the gain medium atoms simply by tuning the pump power. This is an attractive property, which, for example, could be employed to simulate some of the novel aspects of the recently proposed (for their potential ultranarrow linewidths) but technically challenging to realize high-finesse lasers that utilize transitions of alkaline-earth atoms with extremely small dipole moments [2]. Particular interest would be towards investigating the resulting phenomenon of steady-state superradiance [3].

The use of an atomic Raman gain medium for a laser was first demonstrated with a heated vapor cell [4], and has since been realized with cold atoms [5,6]. These experiments show narrow gain bandwidth properties, but operate with low-finesse optical cavities, in a regime where the single-atom cooperativity parameter $C \ll 1$. This parameter is a measure of the effect atoms have on the cavity field, with $C > 1$ indicating a substantial influence even from single atoms.

Here we report the realization of a continuous wave (cw) Raman laser using a magneto-optically trapped (MOT) cloud of ^{87}Rb atoms as the Raman gain medium at the center of a high-finesse, standing wave optical cavity operating in a regime where $C \approx 1$. For our laser, this regime manifests itself with strong nonlinearities in the gain properties even at 100 pW output levels. The nonlinearities result in an atypical lasing threshold behavior involving jumps in the lasing power. We propose a simple model that explains the observed effects. We also measure the intermode laser linewidth, and observe values as low as 80 Hz half-width-half-maximum (HWHM).

In our apparatus, atoms loaded into the MOT at the center of the optical cavity undergo a two-photon Raman transition driven by a frequency tunable pump laser which excites the atoms from the $F = 2$ hyperfine ground state to an intermediate virtual state. An allowed cavity resonance from this intermediate state down to the $F = 1$ hyperfine ground state allows completion of the two-photon process. The atoms are driven back to $F = 2$ by the repump light associated with the MOT, allowing continuous laser output. The relevant atomic energy levels and laser frequencies are shown in Fig. 1(a). We can excite different spatial modes of the cavity, as shown in Fig. 1(b), by tuning the frequency of the Raman pump to select the cavity mode whose frequency satisfies the overall two-photon resonance condition.

The entire apparatus required to achieve lasing has a compact form factor of ~ 0.1 m^3, suitable for a practical laser system. The tubes holding the cavity mirrors are integrated into the MOT chamber, and the entire assembly is constructed from Zerodur, which has a near-to-zero thermal expansion coefficient (2×10^{-8} K^{-1}) at room temperature. The pressure in the chamber is $<10^{-9}$ mbar. Two 10 cm radius-of-curvature mirrors form the cavity in a near-confocal configuration with a separation of $L = 10.7$ cm, resulting in a 110 μm beam waist for 780 nm light at the position of the atoms. The mirror coating is commercially available from Research Electro-Optics, and is highly reflective at 780 and 1560 nm, resulting in measured cavity linewidths of $\kappa_{780} = 2\pi \times 4$ kHz and $\kappa_{1560} = 2\pi \times 6$ kHz. The single-photon Rabi frequency $g_0 = 2\pi \times 140$ kHz results in a single-atom cooperativity $C = g_0^2/(\Gamma\kappa_{780}) = 0.84$, where Γ is the natural linewidth of the ^{87}Rb D_2 transition. For the detunings Δ used in this experiment the resulting atom-induced cavity resonance shifts are $\sim$10–20 Hz/atom. For our cavity parameters, the spacing between nearest sets of transverse modes is

$\Delta\nu_{\mathrm{tms}} = 75$ MHz, much greater than the gain bandwidth of $\sim$3 MHz (γ_{21} below).

A schematic of the experimental setup is shown in Fig. 1(c). The input laser light at 1560 nm is split by a polarizing beam splitter, with one path used to stabilize the frequency of the light to the cavity using a Pound-Drever-Hall (PDH) method [7], to better than a kilohertz. The majority of the light goes in the other path, where it is frequency doubled in a periodically poled lithium niobate (PPLN) waveguide crystal to generate the 780 nm light used for the Raman pump laser and the local oscillator beam. This way of generating the 780 nm light ensures that the Raman transition is insensitive to cavity length drifts. A double-passed accousto-optical modulator allows for tuning of the pump beam frequency, enabling fast switching between spatial modes. We note that the linewidth of the Raman pump does not need to be narrow, as we observe lasing equally well with a MHz linewidth pump.

Light emitted from one cavity mirror is split by a polarizing beam splitter. One beam is incident on a CCD camera to image the spatial mode intensity profile, while the other is incident on a single mode fiber connected to a Perkin-Elmer ARQH-13 avalanche photodiode single-photon counting module (SPCM). Short pulses from the SPCM, corresponding to a photon detection, are integrated, and a time trace is measured on an oscilloscope. Light emitted from the other cavity mirror is combined with a local oscillator beam and incident on a fast photodiode. The resulting beat note gives us the laser's optical frequency relative to the known local oscillator frequency.

We demonstrate a lasing threshold by varying the number of atoms (gain) in the lasing mode. Allowing the MOT to load while keeping the pump intensity constant results in a visible threshold after which lasing occurs. The effective atom number N_{eff} in the cavity mode is related to the actual atom number by a geometrical overlap factor between the MOT cloud and the cavity mode. Figure 2(a) shows a parametric plot of the measured N_{eff} and lasing power for the TEM_{00} mode.

We extract the laser's intermode linewidth, which is insensitive to cavity length fluctuations, from the beat note between two lasing modes. Specifically, by tuning the pump frequency we make the TEM_{01} and TEM_{10} modes lase simultaneously [Fig. 1(b)], and partially couple

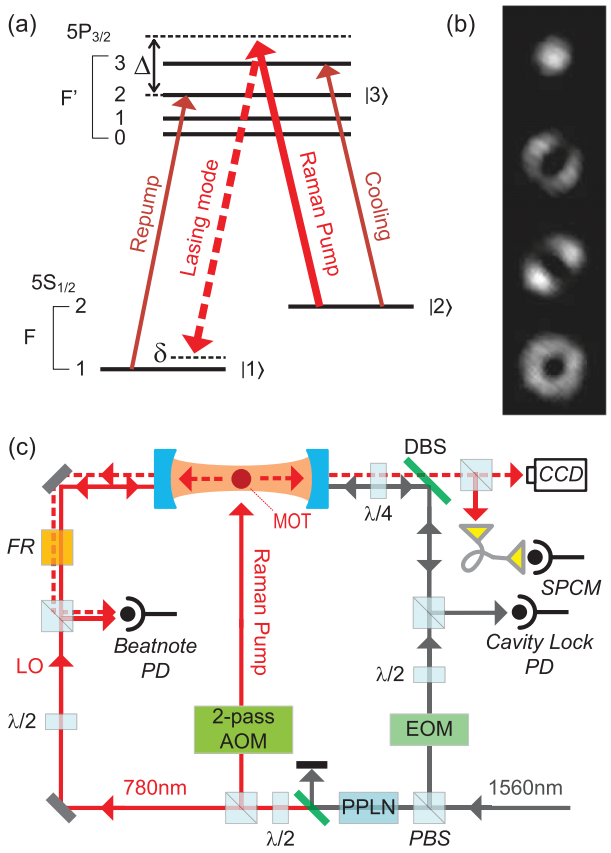

FIG. 1 (color). (a) Energy level diagram of ^{87}Rb including relevant laser frequencies for the Raman process, as well as the cooling and repump light frequencies associated with the magneto-optical trap. (b) Sample CCD images showing relevant spatial modes of the laser. Top to bottom: TEM_{00}, TEM_{01}, TEM_{10}, $\mathrm{TEM}_{01} + \mathrm{TEM}_{10}$, respectively. (c) Schematic of the experiment. LO = local oscillator, AOM = acousto-optical modulator, EOM = electro-optical modulator, FR = Faraday rotator, PBS = polarizing beam splitter, DBS = dichroic beam splitter, $\lambda/2$ = half-wave plate, $\lambda/4$ = quarter-wave plate, PD = photodiode.

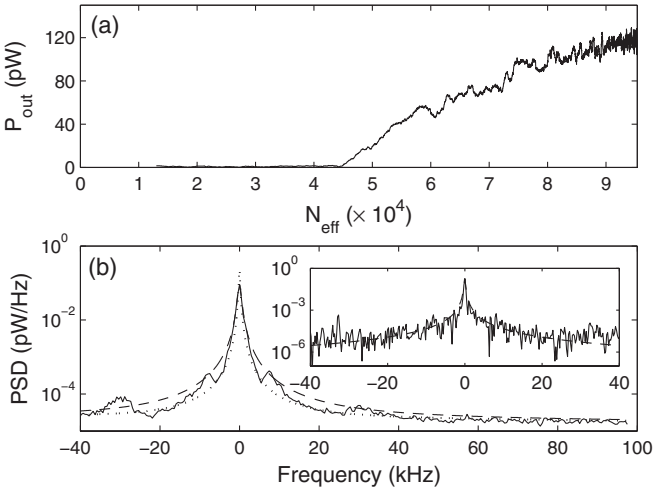

FIG. 2. (a) Cavity output power as a function of N_{eff}. Threshold behavior is clearly visible, indicating the point at which losses at the cavity mirrors are overcome by the gain medium. (b) Measured beat note power spectral density (PSD) between the TEM_{01} and TEM_{10} modes at 25 mW/cm^2 pump intensity with $N_{\mathrm{eff}} = 9 \times 10^4$, showing an average of 100 spectra (2 ms windows) that are centered before averaging. Dashed line: Lorentzian fit with HWHM of 448 Hz, Dotted line: Lorentzian fit to the tails with HWHM of 172 Hz. Inset: A single realization of the spectrum for a particularly stable 4 ms window; dashed line: Lorentzian fit with HWHM of 160 Hz.

these modes into a single mode fiber leading to the SPCM. These two modes are nondegenerate (due to geometrical imperfections in the cavity mirrors) by approximately 515 kHz, a value well within the gain bandwidth. A frequency spectrum extracted from a particularly stable 4 ms window of the recorded time-domain signal is shown in the inset of Fig. 2(b). A Lorentzian fit indicates a HWHM of 160 Hz, corresponding to an instantaneous intermode linewidth of 80 Hz for the convolution of two identical Lorentzian line shapes. Similarly, a minimum average instantaneous intermode linewidth of 224 Hz is obtained by averaging centered spectra derived from consecutive 2 ms windows [Fig. 2(b)]. Note that the purpose of the centering procedure is to eliminate broadening due to central lasing frequency drift. The fact that a good Lorentzian fit to the peak overshoots the tails is an indication of excess low frequency noise on the instantaneous frequency. It is known that the quantum limited linewidth could in principle be inferred from the Lorentzian tails of a line shape at high frequencies [8]. In our case, although small side lobes and a high baseline partly obscure the tails of the distribution, a Lorentzian fit to these tails still represents an upper bound on the quantum limited linewidth of the laser. This procedure yields 86 Hz, and is insensitive to the window size used. Note that this fit necessarily overshoots the peak. Comparison with theory is subtle, but as a reference the Schawlow-Townes linewidth limit (without taking into account amplitude-phase noise coupling, or incomplete population inversion) is 0.25 Hz.

A complete understanding of the line shape and noise sources are beyond the scope of this Letter; however, we would like to point out the following observations. Because of their motion inside of the MOT, the atoms in the lasing modes are expected to get completely replenished within $\sim$1 ms; thus, the difference in the atom numbers seen by the TEM_{01} and TEM_{10} modes could in principle fluctuate significantly in the course of the spectral measurements. As a reference, the shot-noise level is $\sim$150 atoms. Utilizing the measured generic atom number dependences of the absolute lasing frequency [Fig. 3], it can be inferred that only about 20 atoms (well below shot-noise level) of a fluctuation could account for the observed 224 Hz intermode linewidth. Similarly, about 7 atoms of fluctuation accounts for the observed instantaneous intermode linewidth of 80 Hz.

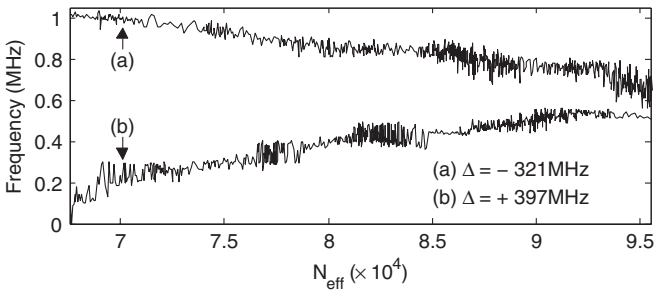

FIG. 3. TEM_{00} lasing mode frequency shift as a function of N_{eff} for (a) red and (b) blue detuned light. Opposite slopes are due to the positive and negative susceptibilities associated with the red and blue detuned configurations, respectively. Relative positioning of the two curves is arbitrary.

The threshold behavior and linewidth narrowing with respect to κ_{780} shown in Fig. 2 constitute the generic signatures of a laser. However, the rather large cooperativity parameter in combination with the relatively narrow Raman gain bandwidth leads to further interesting nonlinear phenomena in lasing behavior. For certain parameters, as the gain is increased, the onset of lasing occurs with an abrupt jump in lasing power, defying traditional threshold behavior. Figure 4(a) shows lasing power as a function of Raman pump intensity for slightly differing pump frequencies, all with positive single-photon detuning Δ. The different pump frequencies correspond to different two-photon detunings δ shown in Fig. 1(a). The jumping behavior in lasing power is observed for positive δ. As the pump intensity is cycled up and down, the onset and extinction of lasing take place at different pump intensities. When δ is negative, this behavior disappears. A simple mechanism based on the ac Stark shift experienced by the

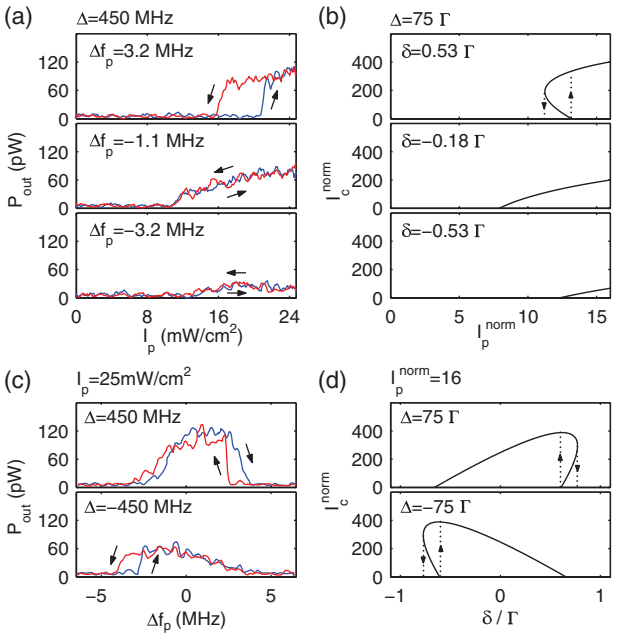

FIG. 4 (color). (a) Cavity output power as a function of pump intensity for different values of the relative pump frequency Δf_p. $\Delta f_p = 0$ is chosen to correspond to the experimentally inferred $\delta = 0$ condition. (b) The corresponding calculated steady-state intracavity intensity. The arrows indicate the expected jumps in the lasing intensity depending on the sweep direction. (c) Cavity output power as a function of Δf_p for opposite single-photon detunings $\pm\Delta$. (d) Calculated steady-state intracavity intensity. Parameters for the calculated curves are $A = 0.135$, $\gamma_{21} = 0.625\Gamma$, $\Gamma_{12} = 0.1\Gamma$.

$F = 1$ state qualitatively captures this effect. For positive Δ, the onset of any lasing will shift the $F = 1$ state up, in turn decreasing δ if it was positive initially, hence increasing the gain which further increases the lasing and the ac Stark shift until equilibrium is reached. For negative δ the ac Stark shift will decrease the gain, resisting the increase in lasing.

The proposed mechanism can be modeled with a three level system [levels $|1\rangle$, $|2\rangle$, $|3\rangle$ in Fig. 1(a)], disregarding the details pertaining to the repump and cooling beams, and taking their effects into account phenomenologically by adding a population transfer rate Γ_{12} from $|1\rangle$ to $|2\rangle$ and additional decoherence rates. The gain associated with an ensemble of atoms can be calculated by solving for the steady-state values of the density matrix elements in a standard fashion [9]. The quantity of interest is the density matrix element ρ_{31} giving the atomic polarization at the lasing transition frequency ω_l, which can be expressed as a sum of one-photon and two-photon terms:

$$\rho_{31}^{(1\mathrm{ph})} = \frac{1}{2(\Delta + i\gamma_{31})}(\rho_{33} - \rho_{11}),$$
$$\rho_{31}^{(2\mathrm{ph})} = \frac{|\Omega_p|^2}{4\Delta^2}\frac{1}{2(-\delta' + i\gamma_{21})}(\rho_{22} - \rho_{11}), \quad (1)$$
$$\rho_{31} = [\rho_{31}^{(1\mathrm{ph})} + \rho_{31}^{(2\mathrm{ph})}]\Omega_c e^{i\omega_l t}.$$

Here $(\rho_{33} - \rho_{11})$ and $(\rho_{22} - \rho_{11})$ are population differences, γ_{31} and γ_{21} are coherence decay rates, Ω_p and Ω_c are the Rabi frequencies associated with the pump and cavity lasing transitions, $\delta' = \delta - (\delta_{ac1} - \delta_{ac2})$ is the effective two-photon detuning with $\delta_{ac1} = \frac{|\Omega_c|^2}{4\Delta}$, $\delta_{ac2} = \frac{|\Omega_p|^2}{4\Delta}$ being the ac Stark shifts, and $(\rho_{22} - \rho_{11}) = 1/(1 + s)$ with $s = \frac{\gamma_{21}}{\Gamma_{12}}\frac{|\Omega|^2}{\delta'^2 + \gamma_{21}^2}$ given in terms of the two-photon Rabi frequency $\Omega = -\frac{\Omega_p^* \Omega_c}{2\Delta}$. In solving the density matrix equations we utilize simplifying assumptions based on $\Delta \gg \gamma_{ij}, \Gamma_{ij}, \delta$. The imaginary part of the expression in square brackets is proportional to the gain or loss, the real part to the phase shift imparted [9].

At this stage, a self-consistent solution to the lasing intensity can be found by equating the single pass gain to the mirror transmission. For the relevant parameter space, $\rho_{31}^{(2\mathrm{ph})}$ brings gain while $\rho_{31}^{(1\mathrm{ph})}$ brings absorption but can be ignored. The resulting equation has the form $AI_p^{\mathrm{norm}} = (1 + \delta'^2/\gamma_{21}^2)(1 + s)$, with δ' and s expressed in terms of the normalized pump and intracavity intensity parameters $I_p^{\mathrm{norm}} = 2|\Omega_p|^2/\Gamma^2$ and $I_c^{\mathrm{norm}} = 2|\Omega_c|^2/\Gamma^2$. Here $A = CN_{\mathrm{eff}}(\Gamma^2/4\Delta^2)(\Gamma/\gamma_{21})$ is a constant depending on various system parameters including cooperativity C, and $\Gamma = \Gamma_{31} + \Gamma_{32}$. The results, for parameters chosen to represent the experiment, are shown in Figs. 4(b) and 4(d), indicating a bistable behavior for certain parameters, closely mimicking the experimental results. Shown in Fig. 4(c) are experimental results of the lasing profile as a function of pump frequency, conforming to the theoretical model. Additional measurements analogous to the ones in Fig. 4(a), but with $\Delta = -450$ MHz indicate that, in this case the roles of positive and negative δ are swapped, as expected.

In summary, we have demonstrated a high-finesse cavity Raman laser using cold atoms as the gain medium. We have observed and explained the emerging nonlinear lasing threshold behavior. Finally, we have measured intermode linewidths as low as 80 Hz between two simultaneously lasing modes, which is of importance for applications like potential ring laser gyroscopes [10] utilizing exotic gain media [11] for rotation sensing. We can identify a few possible future directions. The effects of normal and anomalous dispersion [1] can be investigated for reduced and enhanced, respectively, sensitivity of lasing frequency to disturbances. The proposals for steady-state superradiance [3] can be investigated by tuning the relative strengths of Ω and Γ_{12}. Measurements of intracavity atom numbers can be pursued. The sharp transitions of Fig. 4(a) can be investigated from a possible sensor application perspective, e.g., for measuring disturbances causing atomic level shifts, with the example of superconducting transition edge sensors [12] in mind. Finally, the nonlinearities in Raman lasing can be further studied for possible quantum noise reduction of the intensity fluctuations to below shot noise [13].

This work was funded by NSSEFF and DTRA. S. Bernon acknowledges support from the Fulbright Foundation. We thank L. Hollberg, M. Holland, and D. Meiser for useful discussions.

*Permanent address: Laboratoire Charles Fabry de l'Institut d'Optique, Paris, France.

[1] G. S. Pati *et al.*, Phys. Rev. Lett. **99**, 133601 (2007).
[2] D. Meiser *et al.*, Phys. Rev. Lett. **102**, 163601 (2009).
[3] D. Meiser and M. J. Holland, Phys. Rev. A **81**, 033847 (2010).
[4] P. Kumar and J. H. Shapiro, Opt. Lett. **10**, 226 (1985).
[5] L. Hilico, C. Fabre, and E. Giacobino, Europhys. Lett. **18**, 685 (1992).
[6] W. Guerin, F. Michaud, and R. Kaiser, Phys. Rev. Lett. **101**, 093002 (2008).
[7] R. W. P. Drever *et al.*, Appl. Phys. B **31**, 97 (1983).
[8] M. P. van Exter, S. J. M. Kuppens, and J. P. Woerdman, IEEE J. Quantum Electron. **28**, 580 (1992).
[9] R. W. Boyd, *Nonlinear Optics* (Academic Press, San Diego, 2003).
[10] W. W. Chow *et al.*, Rev. Mod. Phys. **57**, 61 (1985).
[11] M. S. Shahriar *et al.*, Phys. Rev. A **75**, 053807 (2007).
[12] A. E. Lita, A. J. Miller, and S. W. Nam, Opt. Express **16**, 3032 (2008).
[13] H. Ritsch, M. A. M. Marte, and P. Zoller, Europhys. Lett. **19**, 7 (1992).